Influence of black carbon on the measurement of the specific surface of snow with the near infrared method

Philipp Baumann* *ETH Zurich*

November 22, 2017

Abstract

These experiments investigate different possible errors by measuring the specific surface area (SSA) of snow with the near infrared method. The influence of black carbon on this measurement was disapproved, the theory was therefore validated. It shows that sunlight has no influence on the measurement with the IceCube. Wind drift snow as thin layer on the sample can increase the measured value of the specific surface by a few percent. This could be part of the error, observed in former measurements at SLF. As reference for the measured SSA values with the near infrared method, computer tomography was used to verify the SSA values.

*pbaumann@student.ethz.ch

Contents

1 Introduction

2 Scientific context

The specific surface area (SSA) is the surface of snow grains per mass in units of $m^2\,kg^{-1}$ or over the density of ice in m^{-1}. The physical and chemical interaction of snow with its environment is strongly depending on the SSA of the snow, therefore it is an essential quantity to understand processes in snow and for modelling snow packs [Hagenmuller et al., 2016]. The values can vary from less than 5 $m^2\,kg^{-1}$ for melt-freeze layers and ice crusts up to over 150 $m^2\,kg^{-1}$ for freshly fallen snow [Domine et al., 2007]. The dependence of the albedo on the grain size of the snow in the near infrared was shown by Warren Warren [1982] this wavelength can be used to approximate the SSA of snow:

$$SSA \simeq 3\rho_{ice} r_{eff}$$

Where r_{eff} describes the effective (or optical) radius of snow grains, it can be related to the different grain shapes [Gallet et al., 2011]. A wavelength of 1310 nm can be used to measure the SSA with an accuracy of ±10 % if the SSA is below 60 $m^2\,kg^{-1}$ [Gallet et al., 2009]. Another method to determine the SSA is to scan the snow sample with X-ray computer tomography (μCT) and calculate the SSA and density over the surface based on triangulation method [Hildebrand et al., 1999].

2.1 Aim of the study

In snow samples from Greenland obtained in 2015 a difference of over 50% between the measurements by the infrared method and the one with μCT was observed. The near infrared method always resulted in the higher values. Three theories for this difference have been considered (Schneebeli, pers. com, 2017):

- The first assumption is that this difference derives from the calibration of the near infrared instrument with black carbon (BC) polluted alpine snow, whereas the snow from Greenland is much cleaner. Black carbon (soot) reduces the albedo of snow in the visible range more efficiently than other pollutions from the atmosphere [Hansen and Nazarenko, 2004]. However, in the near infrared BC has in theory little impact on the albedo of snow [Warren, 1982]. In this work, we investigated whether black carbon contamination of artificially produced snow has an impact on the SSA measurement with the near infrared method.

Similar experiments were conducted by Brandt et all in 2011, but they focused on the investigation of the albedo reduction of BC contaminated snow [Brandt et al., 2011] and not the influence of BC in the near infrared.

- Under windy conditions, the sample can be covered with a thin film of drift snow which has a much higher SSA than the substrate. Very thin layers of this high SSA snow could influence the optical measurement whereas the μCT measurements are not influenced. This could explain the higher values of the optical measurements.

- Finally the near infrared measurement could be influenced by surrounding sunlight, if the measurement is not perfectly shielded in the near infrared. This stray light could cause increased SSA values in the field compared to the ones in the lab.

We investigated all three possibilities to see if they could, individually or combined, cause the difference of about 50 % between the μCT measurements and the ones with the near infrared method.

2.2 Theory of snow albedo reduction

A low content (110-860 ppb) of BC increases the absorption of sunlight in snow by 1-5 % depending on the concentration and grain size of the snow. BC is a very efficient absorber, this is amplified by the fact that light is scattered in the snow, thereby the interaction of light and BC is increased. BC accelerates the growth of the grain size, which increases again the absorption of sun light. Larger grains allow the light to penetrate the snow deeper, reducing the surface albedo. In nature, the BC effects are usually masked by other effects. The influence of the BC on the albedo is increasing with the grain size and the albedo is most sensitive on concentrations of BC below 200 ppb. The increase of the albedo caused by BC decreases significantly at wavelengths greater than 700 nm.[Hadley and Kirchstetter, 2012] Artificial snow has round grains, this corresponds to the SNICAR model, which was used by Hardley and Kirchstetter [Hadley and Kirchstetter, 2012]. Also old snow gets rounded by the ageing process, which brings the experiment closer to reality.

3 Methods and Measurements

3.1 Instruments

The snow samples were measured with a near infrared device from A2 Photonic Sensors named IceCube and an X-ray computer tomograph from Scanco Medical named μCT40.

- **IceCube** The IceCube is a commercial instrument from A2 Photonic Sensors from Grenoble in France to measure the SSA of snow using the reflectance in the near-infrared. The instrument consists of a integrating sphere with openings for a laser diode with 1310 nm wavelength, for the snow sample and for an InGaAs diode. The snow sample is directly illuminated by the collimated laser beam. The reflected light is collected by the diode and converted in a voltage signal. This signal is converted into reflectance over a calibration with six certified standards. The SSA is calculated by using a polynomial derived from a radiative transfer model. The system is calibrated by the methane absorption method [A2 , 2011]. With this instrument the SSA can be determined in a range from 5 to 130 $m^2\,kg^{-1}$ with a measurement uncertainty of $\pm 10\%$ in the laboratory and in the field. This instrument is the only one which allows to measure the SSA accurately in the field.

- **Scanco μCT40** The μCT40 is a desk computer tomography system from Scanco [uCT]. The tube which has an energy range from 30 to 70 kV. The detector has a resolution of 2048x256 pixels which results in an upper limit for a voxel of 8 µm side length. It has an automatic sample changer which enables to measure up to 10 samples automatically. The μCT is located in a cold lab of the SLF and it is equipped with a fan which blows cold air in the instrument to control the temperature of the sample. The raw data of the CT is reconstructed to a 3D model by a software tool from Scanco. The voxel size in all of our measurements is 8x8x8 μm^3. This grey scale 3D model needs to be segmented into a binary image by the 3-gaussian curve fit method of Hagenmueller et al [Hagenmuller et al., 2016]. This ensures a reproducible and more objective method to discriminate between ice and air.

3.2 Black carbon influence on SSA

For controlled and reproducible conditions the snow was produced artificially.

3.2.1 Snow production

For this reason a laboratory scale snow maker was built producing snow from water in a tank and bottled, pressurised clean air. It operates in a cold room of the SLF. Further details of this SnowSpray can be found in Appendix A.

For the production of snow ultra pure water (<0.054 µS cm^{-1}), provided by a group from the Paul Scherrer Institut (PSI), was used. To ensure a constant pressure and little pollution, we used bottled air from PanGas, which is filtered with a 10 μm filter. All pipes and the water tank were washed out multiple times before the first production. Brandt received the best results with a formulation from Tokai Corporation Aquablack 162 [Brandt et al., 2011], therefore we used the same black carbon. This soot has been chemically modified to contain polar groups on the surface so it dissolves in water. In nature black carbon concentrations between 0.23 ppb (corresponding to ng g^{-1}) on the South Pole and 482 ppb in the French Alps were reported [Flanner et al., 2007]. Therefore snow with 5 different BC concentrations (0 ppb, 50 ppb, 100 ppb, 500 ppb, 1000 ppb) were produced to cover the whole range of typical BC concentrations. The snow was produced within 2 hours after mixing the concentrations to reduce possible sedimentation. After collecting the snow it was sieved with a grid size of 1 mm and filled into the sample containers for storage.

3.2.2 Measurements

10 samples for each concentraion were produced and stored under isothermal conditions at a temperature of $-8°C$. We measured during 8 weeks one sample per week with both the IceCube and the μCT. All surfaces of containers and tools were cleaned before sample preparation and all work with the samples was done with clean gloves to ensure no contaminations of the snow surface. The IceCube was turned on 30 min before the start of the measurements to let it stabilise. The calibrations with the standards was done before and after the measurements to detect drifts and pollutions of the integration sphere. For the μCT scans an energy of 55 kV and a current of 145 µA was used.

3.3 Ambient light effect

To quantify the possible influence of sunlight on the measured values with the IceCube, measurements in the laboratory, in the sun and in a snow pit were performed. Snow from the same sample was used for all three

measurements to ensure the comparability. The lab measurements were executed in the SLF cold lab at $-23°C$ and $-5°C$, where as the outdoor ones were done in the Fluela valley in the blazing sun at nearly $0°C$ and in a covered pit. The snow was first measured in the μCT, then transported in a styrofoam box to the Fluela valley. After the outdoor measurements another reference CT scan and the lab measurements were undertaken.

3.4 Influence of superficial wind-transported snow dust

To simulate similar conditions as in Greenland, clean snow from the BC experiment was compressed. Snow with a density of 300 $\mathrm{kg\,m^{-3}}$ was sieved (1mm) into sample holders and compressed by a maximal pressure of 274.8 kPa to a density around 400 $\mathrm{kg\,m^{-3}}$. This was done in a press by compressing the snow repeatedly by 1 mm and waiting for 10 min to let the snow relax. This was repeated 14 times and the sample was thereby compressed from 40 mm to 26 mm. To get an even lower SSA, the snow was sintered at -5° C for 8 hours respectively 1 week. The samples were measured in the IceCube and the μCT. To simulate the wind-transported snow dust on the surface, snow was sieved with a 500 μm sieve on the surface of the compressed sample. The thickness of the layer was determined by the additional weight due to the sieved snow. To quantify the properties of this superficial snow, a sample holder was filed with the sieve and measured separately in the IceCube and the μCT. To extrapolate the measurements, the measured data was simulated with model named Two-streAm Radiative TransfEr in Snow (TARTES). In this model, each layer of snow is approximated by the asymptotic solution of the radiative transfer theory [Kokhanovsky and Zege, 2004], where as the albedo for the entire snowpack is calculated by the two-stream approximation [Libois et al., 2013]. He et al [He et al., 2017] proposed an albedo reduction for pure close packed snow at visible wavelength. No studies about the close pack effect in the near infrared could be found.

4 Results and Disscusion

4.1 Black carbon influence on SSA

For the samples measured right after the production (less then 26 hours) in week 0, the SSA values determined by the IceCube were widely spread between 44.1 to 120.2 $\mathrm{m^2kg^{-1}}$ (Table 1).

The snow was still very loose as it can be seen in figure 1b, therefore the sample holder could possibly shine trough and influence the measurement.

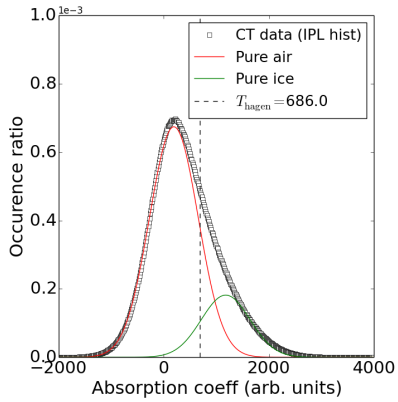

Histogram of new snow (a)

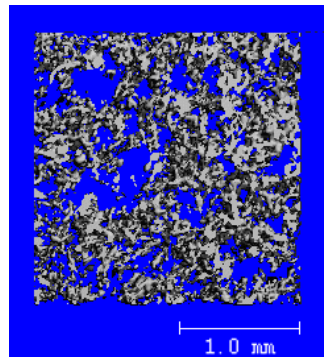

CT image of new snow (b)

Figure 1: Histogram (a) of the grey value 3d CT model and the segmented 3d model of the clean snow 26 hours after production

Concentration of BC in ppb	0	50	100	500	1000
SSA in m^2kg^{-1}	44.1	78.3	106.8	120.2	107.7

Table 1: IceCube SSA values measured within less then 26 hours after production of the snow

With this kind of snow it was not possible to calculate the density and SSA from the CT measurement because the histogram is not clearly separated(fig. 1a).

The snow sintered during the 8 week storage at -8°C and in the histogram the difference between ice and air gets clearer and distinguishable (fig. 2a).

Calculated concentration of BC in ppb	0	50	100	500	1000
Measured concentration of BC in ppb	2.03	9.55	16.7	165.1	333.4

Table 2: Comparison of the calculated and measured black carbon concentration in the snow samples in ppb which is the same as ng/kg.

Samples of the snow were sent to the Paul Scherrer Institut (PSI) to verify the black carbon concentrations. The results of their measurements (Table 2) differ strongly from the calculated values. This difference can be explained by calibration of the instrument at the PSI. This instrument is calibrated with a soot (Aquadag) which has a different grain size distribution than Aquablack. Therefore the measurement is not suitable, however, it

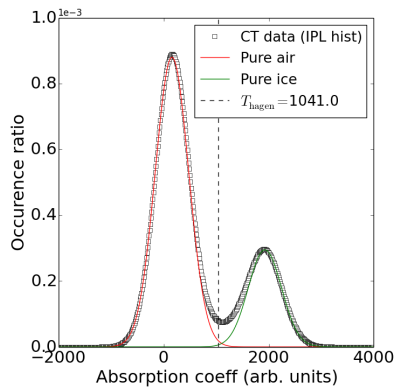

Histogram after eight weeks aging(a)

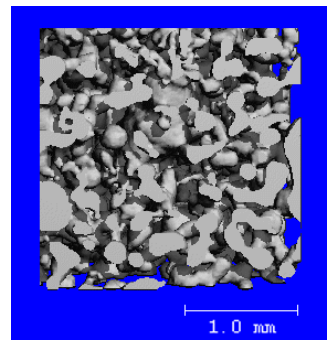

CT image after eight weeks aging(b)

Figure 2: Histogram of the grey value 3d CT model and the segmented 3d model of the clean snow 8 weeks aged at -9°C

proves the order of magnitude of the black carbon concentration.

The density increased over the 8 weeks storage time from around 100 $\mathrm{kg\,m^{-3}}$ up to over 200 $\mathrm{kg\,m^{-3}}$ (Appendix A). All snow samples with different black carbon concentrations showed a similar increase in density.

The SSA exponentially decayed over the 8 weeks storage time due to isothermal metamorphism [Kaempfer and Schneebeli, 2007]. Both methods, IceCube and μCT, showed similar values during the 8 weeks. To compare the SSA of the different concentrations over the 8 weeks the measured values need to be normalised. Therefore the mean over all measurements with different concentrations was calculated for each week.

$$\mathrm{mean}_{\mathrm{IceCube}} = \frac{1}{5} \sum_{concentrations} \mathrm{SSA}_{\mathrm{IceCube}}$$

The same value was calculated for the measurements with the μCT. This mean values were subtracted from the measured values to normalise them and make the values comparable over the 8 weeks. From this normalised values the mean and standard deviation over all weeks from each concentration and each method was calculated and plotted in figure 4. The SSA value of the IceCube dosen't show any significant dependency on the black carbon concentration whereas the μCT shows lower SSA values for lower concentrations.

All samples were produced under the same conditions but they are

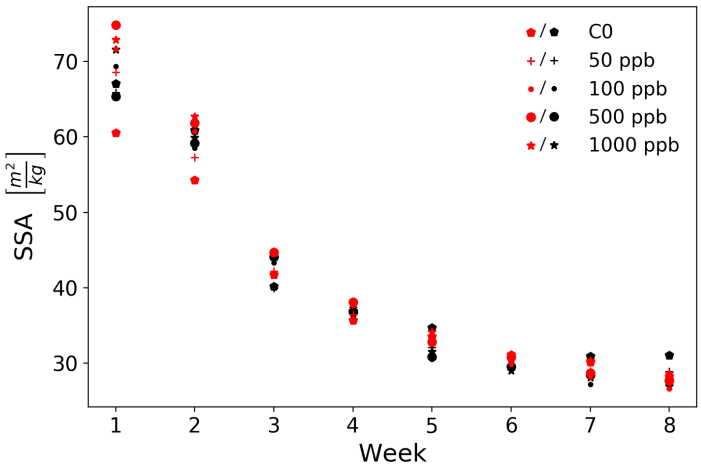

Figure 3: Evolution of the specific surface area measured with the IceCube (black) and the μCT (red) over all ageing stages. The values for the 0 week, up to 26 hours after the production, are not plotted for the reasons mentioned above.

sieved separately, this could cause differences in density and nonhomogeneous shrinking due to edge effect in small storage containers. It is more meaningful to compare the measurements of the two methods.

This can be done in units of $\mathrm{m}^2\,\mathrm{kg}^{-1}$:

$$\mathrm{diff} = \mathrm{SSA}_{IceCube} - \mathrm{SSA}_{\mu CT}$$

or as the relative percentage difference:

$$\mathrm{diff}_r = \frac{100\%}{(\mathrm{SSA}_{IceCube} + \mathrm{SSA}_{\mu CT})/2} * (\mathrm{SSA}_{IceCube} - \mathrm{SSA}_{\mu CT})$$

The difference between the two methods in absolute percent shows that after 2 weeks the μCT and IceCube measured the SSA with a standard deviation of less then 8% shown in Table 3. Over 8 weeks and 5 concentrations the difference of the SSA value measured with the IceCube and μCT is only 1.28% with a standard deviation of 2.28%.

In figure 5 for each BC concentration the relative difference between the SSA value of the IceCube and μCT was taken for every week. The band in the box is the median, the top and bottom of the box are the first and third quartiles and the whiskers represent the 5 respectively the 95 percentiles. No clear trend can be seen neither in figure 4 nor in 5. Under controlled

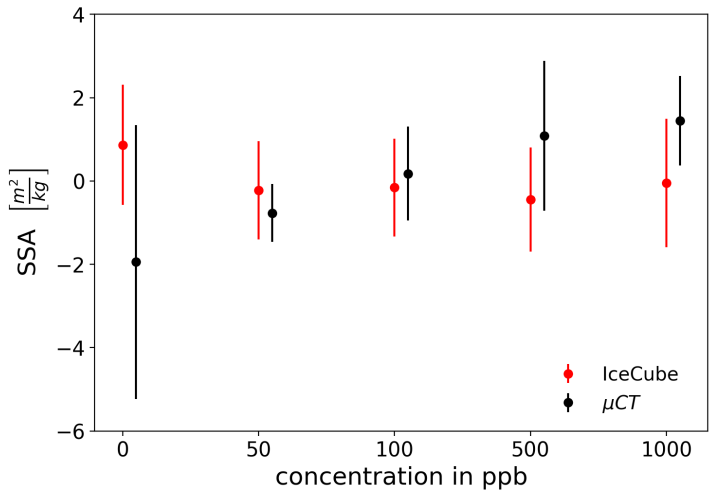

Figure 4: Normalised and averaged SSA values from the IceCube and μCT measurments. The standard deviation is calculated from the 8 values per concentration.

conditions the SSA measurements of the μCT and the ones with the IceCube differ less then 5% with no systematic difference. Therefore black carbon in the snow can not explain the difference of 50% between the two methods, measured in Greenland.

Week	Mean Difference in %	Mean Difference in m^2kg^{-1}
1	-2.14±7.51	-1.84±5.09
2	0.53±6.47	0.12±3.66
3	-4.09±1.91	-1.78±0.84
4	-0.92±3.22	-0.37±1.19
5	-3.75±4.15	-1.24±1.39
6	-2.63±2.63	-0.81±0.81
7	-0.51±4.75	-0.16±1.40
8	3.31±5.64	0.90±1.58
Mean	-1.28±2.28	-0.65±0.89

Table 3: Mean differences over 8 weeks between IceCube and μCT measurments in % and m^2kg^{-1}. The mean of the means gives -1.28±2.28% respectively -0.65±0.89 m^2kg^{-1}.

4.2 Ambient light effect

The data in Table 4 shows the independence of the IceCube measurements from the ambient sunlight and a significant influence of the temperature. The transport ways were short (20 min) and the data of μCT showed no significant change due to the transport. The standard deviation over the different measurements under the same condition is the most changing value between in- and outdoor. This is caused by the more comfortable and constant sample preparation in the lab.

Device and location	SSA, m^2kg^{-1}
μCT before	39.2
IceCube Fluela Sun	38.7±2.0
IceCube Fluela snow pit	38.1±2.0
IceCube Lab @ $-5°C$	40.5±0.3
IceCube Lab @ $-23°C$	38.1±0.1
μCT after	37.4

Table 4: Comparison of the SSA values, measured with the IceCube at different locations and as reference with the μCT. The values of the IceCube are mean values of 5 different samples from the same snow under the same conditions.

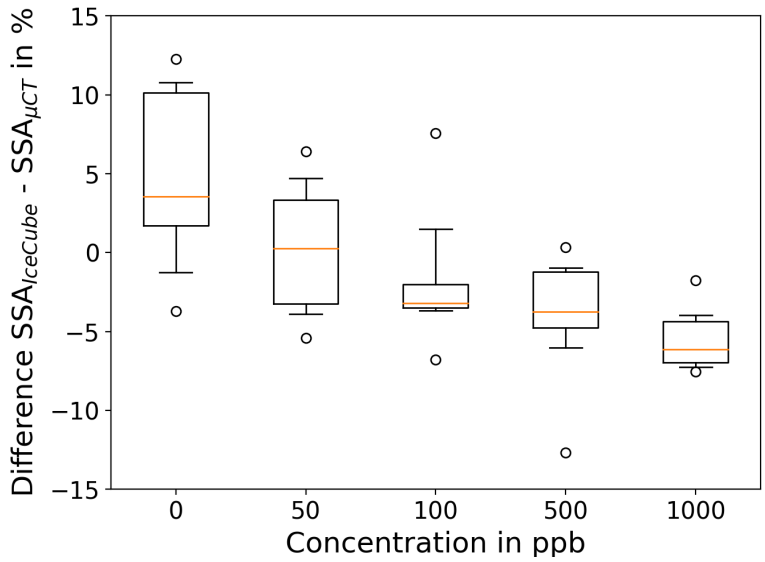

Figure 5: Relative percentage difference (diff_r) as boxplot per concentration over 8 weeks.

4.3 Influence of superficial wind-transported snow dust

In figure 6 SSA values, measured with the IceCube, of compressed and sintered substrate with superficial layers of high SSA snow are shown. The substrate of the blue data is sintered for 8 hours, where as the red data for 1 week, both at -5° C. The thickness of the layer varies from 0.1 mm up to 3.5 mm. In addition, this plot shows data simulated by TARTES. As parameters for the simulation SSA value for the dense snow of 36 $m^2\,kg^{-1}$ respectively 32 $m^2\,kg^{-1}$ and for the high SSA snow of 56.5 $m^2\,kg^{-1}$ respectively 54 $m^2\,kg^{-1}$ fitted the best. Those values are close to the ones measured by the μCT.

Whit this parameters more extreme combinations of SSA values can be simulated. In figure 7 snow with SSA values up to 150 $m^2\,kg^{-1}$ and density of 200 respectively 100 $kg\,m^{-3}$ on a substrate with a density of 500 $kg\,m^{-3}$ and a SSA of 30 $m^2\,kg^{-1}$ is simulated. This simulation shows that even thin layers with an thickness of less then 0.5 mm of dense, high SSA snow can increase the measured SSA value more then 50 %.

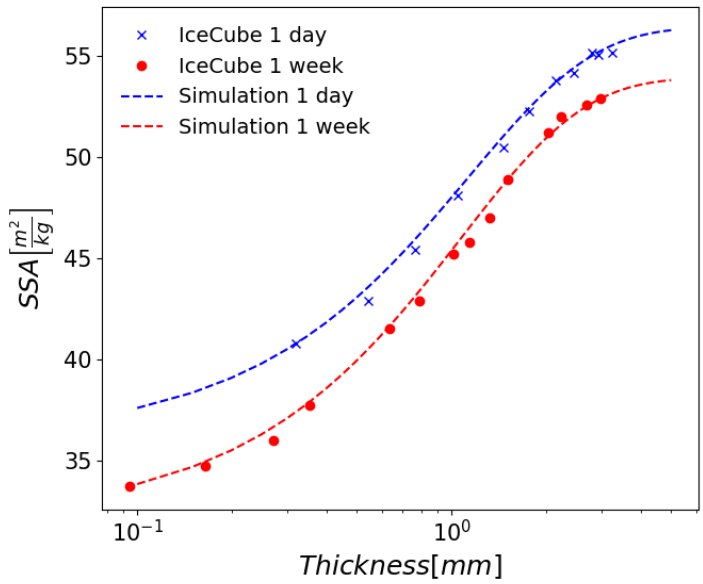

Figure 6: SSA measured with IceCube of a compressed and sintered substrate with superficial layers of high SSA snow. The dotted lines are simulated with TARTES.

5 Conclusion and outlook

No influence of black carbon on the albedo of snow in the near-infrared could be observed in our experiments. It could also be shown that ambient light has no influence on the measurements with the IceCube. However layer of wind drift snow can have an influence on the SSA value measured with IceCube, under extreme conditions it can increase the measured value up to 50% even for thin layers. More investigations need to be done on the density dependency of the SSA measurement with the IceCube.

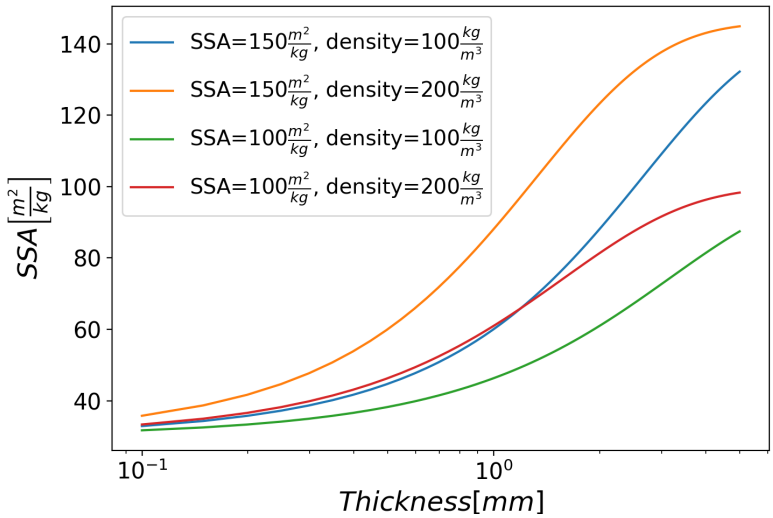

Figure 7: TARTES simulations for superficial layers of different SSA values and densities and a substrate with a density of 500 $\mathrm{kg\,m^{-3}}$ and a SSA of 30 $\mathrm{m^2\,kg^{-1}}$

6 Acknowledgement

Special thanks goes to Dr. Martin Schneebeli who offered me the possibility to write this Semesterarbeit at the WSL Institute for Snow and Avalanche Research SLF and supported me in scientific and methodic regards. I also appreciate the technical support of Matthias Jaggi. Special thanks to Franziska Roth, who supported me in the μCT measurements and Juerg Trachsel, who helped me with the IceCube measurements and snow production. Another thank goes to Professor Christoph Grab for supervising me.

References

IceCube Innovative optical system for measuring the specific surface area (SSA) of snow. A2 Photonic Sensors, 3, Parvis Louis Néel - BP 257 38016 Grenoble cedex 1, FRANCE, 1.5 edition, July 2011.

R. E. Brandt, S. G. Warren, and A. D. Clarke. A controlled snowmaking experiment testing the relation between black carbon content and reduction of snow albedo. *Journal of Geophysical Research*, 116(D08109), 2011. doi: 10.1029/2010JD015330.

F. Domine, A. S. Taillandier, and W. R. Simpson. A parameterization of the specific surface area of seasonal snow for field use and for models of snowpack evolution. *Journal of Geophysical Research*, 112:F02031, 2007. doi: 10.1029/2006JF000512. URL `http://dx.doi.org/10.1029/2006JF000512`.

M. G. Flanner, C. S. Zender, J. T. Randerson, and P. J. Rasch. Present-day climate forcing and response from black carbon in snow. *Journal of Geophysical Research*, 112:D11202, 2007. doi: 10.1029/2006JD008003.

J.-C. Gallet, F. Domine, C. S. Zender, and G. Picard. Measurement of the specific surface area of snow using infrared reflectance in an integrating sphere at 1310 and 1550—[thinsp]—nm. *The Cryosphere*, 3:167–182, 2009. doi: 10.5194/tc-3-167-2009.

J.-C. Gallet, F. Domine, L. Arnaud, G. Picard, and J. Savarino. Vertical profile of the specific surface area and density of the snow at dome c and on a transect to dumont d'urville, antarctica - albedo calculations and comparison to remote sensing products. *The Cryosphere*, 5:631–649, Sept. 2011. doi: 10.5194/TCD-4-1647-2010. URL `https://hal.archives-ouvertes.fr/hal-00561262`.

O. L. Hadley and T. W. Kirchstetter. Black-carbon reduction of snow albedo. *Nature Climate Change*, 2(6):437–440, 06 2012. doi: 10.1038/nclimate1433. URL `http://dx.doi.org/10.1038/nclimate1433`.

P. Hagenmuller, M. Matzl, G. Chambon, and M. Schneebeli. Sensitivity of snow density and specific surface area measured by microtomography to different image processing algorithms. *The*

Cryosphere, 10(3):1039–1054, 2016. doi: 10.5194/tc-10-1039-2016. URL `http://www.the-cryosphere.net/10/1039/2016/`.

J. Hansen and L. Nazarenko. Soot climate forcing via snow and ice albedos. *Proceedings of the National Academy of Sciences of the United States of America*, 101(2):423–428, 2004. doi: 10.1073/pnas.2237157100.

C. He, Y. Takano, and K.-N. Liou. Close packing effects on clean and dirty snow albedo and associated climatic implications. *Geophysical Research Letters*, 44(8):3719–3727, 2017.

T. Hildebrand, A. Laib, R. Müller, J. Dequeker, and P. Rüegsegger. Direct three-dimensional morphometric analysis of human cancellous bone: microstructural data from spine, femur, iliac crest, and calcaneus. *Journal of bone and mineral research*, 14(7):1167–1174, 1999. doi: 10.1359/jbmr.1999.14.7.1167.

T. U. Kaempfer and M. Schneebeli. Observation of isothermal metamorphism of new snow and interpretation as a sintering process. *Journal of Geophysical Research*, 112(D24101), 2007. doi: 10.1029/2007JD009047.

A. A. Kokhanovsky and E. P. Zege. Scattering optics of snow. *Appl. Opt.*, 43(7):1589–1602, Mar 2004. doi: 10.1364/AO.43.001589. URL `http://ao.osa.org/abstract.cfm?URI=ao-43-7-1589`.

Q. Libois, G. Picard, J. France, L. Arnaud, M. Dumont, C. Carmagnola, and M. King. Influence of grain shape on light penetration in snow. *The Cryosphere*, 7(6):1803–1818, 2013. doi: 10.5194/tc-7-1803-2013.

S. G. Warren. Optical properties of snow. *Reviews of Geophysics*, 20(1):67–89, 1982. doi: 10.1029/RG020i001p00067. URL `http://dx.doi.org/10.1029/RG020i001p00067`.

Appendices

A Appendix

Container ID	Prod Date	Gross [g]	Tara [g]	Net[g]	Storage Condition	Experiment Date	SSA IceCube[	SSA uCT	Density uCT	Measured BC	CT Sample#	Measurment#	File#	Trashold (Hagenm.)
C01	04.04.17 ?				26h @-23°C	05.04.17	44.1			2.027	1603	4159	3966	
C02	04.04.17	68.2	25.79	42.41	1 weeke @ -8°C	12.04.17	67.1	60.57	142.9	2.027	1613	4187	3994	1004
C03	04.04.17	67.1	25.77	41.33	2 weeks @-8°C	19.04.17	60.9	54.25	168	2.027	1622	4209	4016	1018
C04	04.04.17	62.5	26.22	36.28	3 weeks @-8°C	26.04.17	40.2	41.75	207	2.027	1630	4221	4028	1021
C05	04.04.17	69.4	26.2	43.2	4 weeks @-8°C	03.05.17	36.9	35.67	222.6	2.027	1641	4259	4066	1024
C06	04.04.17	68.73	25.77	42.96	5 weeks @-8°C	10.05.17	34.7	33.48	224.3	2.027	1661	4322	4127	1037
C07	04.04.17	68.43	26.28	42.15	6 weeks @-8°C	17.05.17	30.7	31.09	232.4	2.027	1673	4349	4147	1016
C08	04.04.17	69.48	26.25	43.23	7 weeks @-8°C	24.05.17	30.9	30.09	225.6	2.027	1682	4382	4180	1031
C09	04.04.17	66.6	25.75	40.85	8 weeks @-8°C	31.05.17	31	28.2	242.6	2.027	1694	4403	4194	1041
C10	04.04.17	68.52	25.82	42.7	8 weeks @-23°C	30.05.17	47.5	42.59	186.2	2.027	1687	4387	4185	997
50ppb1	04.04.17 ?				23h @-23°C	05.04.17	78.3			9.549	1604	4162	3969	
50ppb2	04.04.17	57.52	26.21	31.31	1 weeke @ -8°C	12.04.17	65.9	68.56	106.2	9.549	1612	4186	3993	975
50ppb3	04.04.17	69.3	25.8	43.5	2 weeks @-8°C	19.04.17	58.9	57.26	157	9.549	1623	4210	4017	1052
50ppb4	04.04.17	58.6	25.65	32.95	3 weeks @-8°C	26.04.17	39.9	42.18	183.4	9.549	1631	4223	4030	1034
50ppb5	04.04.17	58.5	25.72	32.78	4 weeks @-8°C	03.05.17	37.4	36.47	205.8	9.549	1642	4260	4067	1024
50ppb6	04.04.17	57.8	25.8	32	5 weeks @-8°C	10.05.17	32.1	32.77	235.7	9.549	1662	4323	4128	1047
50ppb7	04.04.17	58.94	26.21	32.73	6 weeks @-8°C	17.05.17	29.8	30.73	220.5	9.549	1674	4350	4148	1036
50ppb8	04.04.17	59.3	26.27	33.03	7 weeks @-8°C	24.05.17	30.8	28.94	230	9.549	1683	4383	4181	1033
50ppb9	04.04.17	58.2	26.21	31.99	8 weeks @-8°C	31.05.17	28.9	27.6	232.6	9.549	1695	4404	4195	1032
50ppb10	04.04.17	58.2	25.81	32.39	8 weeks @-23°C	30.05.17	43.6	43.45	178.8	9.549	1688	4388	4186	1036
100ppb1	05.04.17 ?				10h @-23°C	05.04.17	106.8			16.734	1605	4163	3970	
100ppb2	05.04.17	55.12	26.22	28.9	1 weeke @ -8°C	12.04.17	69.4	71.69	113.9	16.734	1614	4188	3995	1001
100ppb3	05.04.17	53.3	25.79	27.51	2 weeks @-8°C	19.04.17	58.5	60.73	130	16.734	1624	4211	4018	1029
100ppb4	05.04.17	51.7	25.77	25.93	3 weeks @-8°C	26.04.17	43.3	44.72	184.7	16.734	1632	4225	4032	1034
100ppb5	05.04.17	53.9	26.25	27.65	4 weeks @-8°C	03.05.17	36.4	37.62	174.1	16.734	1645	4261	4068	1033
100ppb6	05.04.17	53.2	26.26	26.94	5 weeks @-8°C	10.05.17	30.5	32.72	194.7	16.734	1663	4324	4129	1031
100ppb7	05.04.17	53.43	26.25	27.18	6 weeks @-8°C	17.05.17	30.3	29.85	350.1	16.734	1675	4351	4149	1081
100ppb8	05.04.17	55.08	26.18	28.9	7 weeks @-8°C	24.05.17	27.2	28.17	240.9	16.734	1684	4384	4182	1033
100ppb9	05.04.17	50.23	25.75	24.48	8 weeks @-8°C	31.05.17	28.6	26.59	244.4	16.734	1696	4405	4195	1033
100ppb10	05.04.17	54.36	25.74	28.62	8 weeks @-23°C	30.05.17	45.5	44.61	173.9	16.734	1689	4389	4187	1035
500ppb1	05.04.17 ?				6h @-23°C	05.04.17	120.2			165.065	1606	4166	3973	
500ppb2	05.04.17	52.22	25.77	26.45	1 weeke @ -8°C	12.04.17	65.4	74.88	101.6	165.065	1615	4189	3996	1008
500ppb3	05.04.17	49.5	26.25	23.25	2 weeks @-8°C	19.04.17	59.2	61.87	135.5	165.065	1627	4214	4021	1060
500ppb4	05.04.17	52	26.13	25.87	3 weeks @-8°C	26.04.17	44.1	44.68	161.4	165.065	1633	4226	4033	1038
500ppb5	05.04.17	49.8	26.13	23.67	4 weeks @-8°C	03.05.17	36.8	38.1	201.3	165.065	1646	4262	4069	1039
500ppb6	05.04.17	50.8	25.71	25.09	5 weeks @-8°C	10.05.17	30.8	32.77	199.3	165.065	1664	4325	4130	1038
500ppb7	05.04.17	51.1	26.63	24.47	6 weeks @-8°C	17.05.17	29.5	30.75	198.7	165.065	1676	4352	4150	1031
500ppb8	05.04.17	51.99	25.69	26.3	7 weeks @-8°C	24.05.17	28.4	28.68	216.6	165.065	1685	4385	4183	1034
500ppb9	05.04.17	48.41	26.17	22.24	8 weeks @-8°C	31.05.17	27.7	27.61	236.8	165.065	1697	4406	4196	1037
500ppb10	05.04.17	51.25	26.14	25.11	8 weeks @-23°C	30.05.17	43.9	43.78	165.1	165.065	1690	4394	4191	996.7
1000ppb1	05.04.17 ?				2h @-23°C	05.04.17	107.7			333.489	1607	4167	3974	
1000ppb2	05.04.17	49.93	26.23	23.7	1 weeke @ -8°C	12.04.17	71.6	72.88	90.3	333.489	1616	4190	3997	1009
1000ppb3	05.04.17	52.6	26.22	26.38	2 weeks @-8°C	19.04.17	59.9	62.71	128.4	333.489	1626	4213	4020	1054
1000ppb4	05.04.17	50.7	25.63	25.07	3 weeks @-8°C	26.04.17	41.7	44.78	174.1	333.489	1634	4227	4034	1039
1000ppb5	05.04.17	49.9	25.67	24.23	4 weeks @-8°C	03.05.17	36.4	37.9	199.3	333.489	1647	4263	4070	1040
1000ppb6	05.04.17	50.06	25.62	24.44	5 weeks @-8°C	10.05.17	31.5	34.07	203.9	333.489	1665	4326	4131	1035
1000ppb7	05.04.17	51.33	26.24	25.09	6 weeks @-8°C	17.05.17	29	30.95	222.4	333.489	1677	4353	4151	1035
1000ppb8	05.04.17	52.5	25.73	26.77	7 weeks @-8°C	24.05.17	28.1	30.3	221.1	333.489	1686	4386	4184	1034
1000ppb9	05.04.17	51.61	25.76	25.85	8 weeks @-8°C	31.05.17	26.9	28.61	215.8	333.489	1698	4407	4198	1026
1000ppb10	05.04.17	49.13	26.24	22.89	8 weeks @-23°C	30.05.17	43.5	45.08	181.2	333.489	1691	4391	4188	1039

B Appendix

SnowSprayer
A labor scale snow machine

Philipp Baumann* *ETH Zurich Semesterarbeit SLF*

August 28, 2017

Contents

*pbaumann@student.ethz.ch

1 Function principal

This SnowSprayer produces rounded, fin grained snow with a two media nozzle. The nozzle mixes water and pressurised air, of which the water has the higher pressure. In figure 1 the mixing nozzle and the very different diameters of water and air can be seen. Through the expansion of the air, the water is cooled and down gets frozen. The volumetric current of the

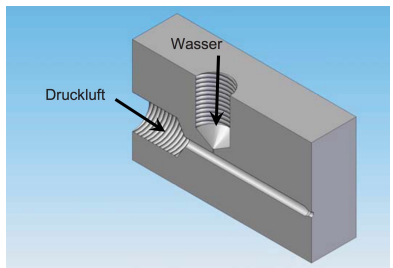

Figure 1: sketch of the nozzle [1]

air is four times the one of the water with this nozzle [1]. The drop size distribution can be seen in figure 2.

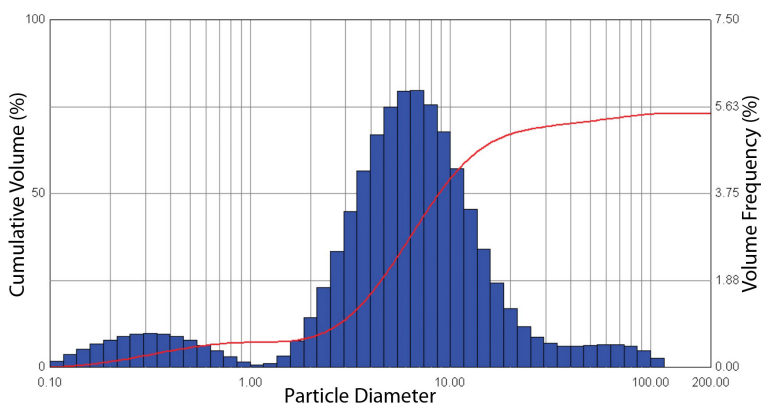

Figure 2: blue: cumulative volume per drop size, red: volume frequency of the drop size [1]

2 Setup

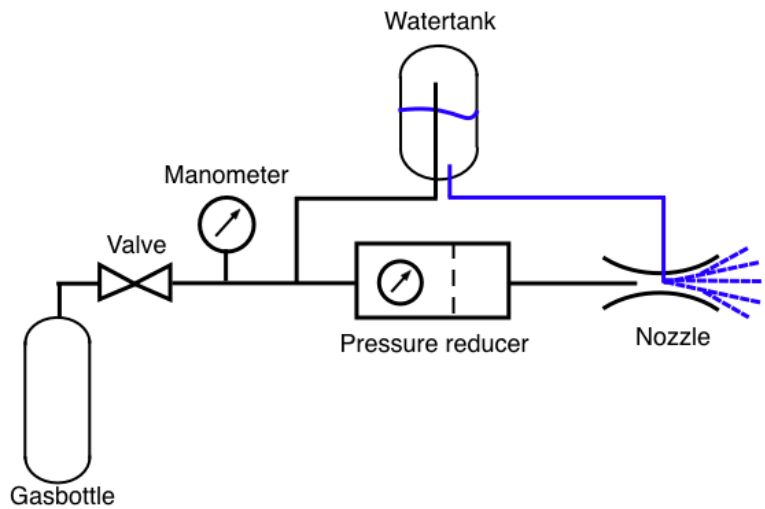

Figure 3: schema of the setup in the cold lab of the SLF

The system is driven by only one pressure source, a gas bottle. Bottled air is used to guarantee clean and oil free air for the snow production and to supply the nozzle with $V_n/t = 200l/min$ at a pressure of $8bar$. By a pressure reduction valve a constant pressure can be provided. The air is guided in insulated pipes into the cold lab where one part of the air pressurises a tank with water and the other one is again reduced in pressure. Both lines are recombined in the nozzle (fig. 1 All pipes with water, the nozzle and the water tank are insulated and heated to avoid freezing (fig. 4).

Figure 4: Styrofoam box of the tank with all pipes connected

3 Preparations

Before the snow production the tank needs to be filled with water and possible additions like black carbon. This can be done with a can containing the water on the top of the styrofoam box and short pipes like in figure 5. In the cold the air pipe and the electrical power for the heating needs to be prepared. To prevent the cooling system of the cold lab from freezing, a curtain needs to be spanned to shield the water vapour and the fine snow in the air (fig. 6) from the fans of the cooling system.

Figure 5: filling of the tank with black carbon contaminated water

4 Snow production

The tank with the mounted nozzle has to be brought right before the start of the production into the cold lab. The main pressure on the gas bottle has to be set to 8 bar. The pressure reduction at the tank should have 6.5 bar. To turn on and off the production the whole tank has to be flipped upside down. If the pressure is turned off during production, the residual air in the tank would press the water out. This would destroy the whole produced snow.

The nozzle needs to be controlled every 10 minutes to prevent it from freezing. Ice on the nozzle can block the air stream and stopp the production. To stop the snow production before all water is used, the tank has to be flipped upside down. After the production the tank and nozzle needs to be brought outside of the cool lab to prevent the rest water from freezing. The new snow has to be collected and filled into the storage containers.

Figure 6: SnowSprayer in operation

References

[1] Daniela Lehner , *Vorversuche mit verschiedenen luftgestuetzten Zerstaeubern*, 2008, FHNW